Journal of Applied Physics ARTICLE scitation.org/journal/jap

Dipole radiation near a reflecting corner

Cite as: J. Appl. Phys. **127**, 083101 (2020); doi: 10.1063/1.5140744
Submitted: 30 November 2019 · Accepted: 10 February 2020 ·
Published Online: 25 February 2020

Henk F. Arnoldus,[1,a] Zhangjin Xu,[1,b] and Xin Li[2,c]

AFFILIATIONS

[1]Department of Physics and Astronomy, Mississippi State University, P.O. Box 5167, Mississippi State, Mississippi 39762-5167, USA
[2]Department of Physics, Millersville University, P. O. Box 1002, Millersville, Pennsylvania 17551-1002, USA

[a]**Author to whom correspondence should be addressed:** hfa1@msstate.edu
[b]**E-mail:** zx47@msstate.edu
[c]**E-mail:** Xin.Li@millersville.edu

ABSTRACT

We consider a radiating electric dipole, located near the joint of two orthogonal mirrors. The field lines of energy flow in the neighborhood of the dipole have an intriguing structure due to interference between the dipole radiation and the reflected light by the mirrors. Numerous singularities and vortices appear in the sub-wavelength region between the dipole and the surfaces. We present a method to find the locations of the vortices and singularities without regard to the details of the flow pattern. The radiation field induces a surface current density in the mirrors. The direction of the current is predominantly in the radial direction for a linear dipole, but it alternates between outgoing and incoming across singular curves. We show that the field line pattern expands with a phase velocity larger than the speed of light. For a circular dipole, there appears a spiral which runs inward. The current initially flows in along this spiral. Then the current leaves again along an outgoing spiral, which spirals inside the incoming spiral. Current can flow from one mirror to the other, and we show that the current always crosses the intersection line at a 90° angle.

I. INTRODUCTION

The rapid development of nanotechnology and nano-photonics over the last few decades have made it paramount to study optical phenomena on a scale of a wavelength or even smaller. Ray diagrams cannot account for the interactions between nanoparticles and, for instance, a nearby substrate. Radiative emission rates of atoms, molecules, and microparticles are affected by a nearby material medium, as was observed for the first time by Drexhage[1] in his landmark experiments with molecular dyes deposited on a dielectric material. The influence on molecular emission rates was studied theoretically in Ref. 2, and the predictions correspond very well with the experimental results. The recent advances in metamaterial design have opened an entirely new field of nano-optics. Negative-index-of-refraction materials have been predicted to possibly have the ability of focusing light tighter than the diffraction limit,[3] and epsilon-near-zero metamaterials may provide a way to optically levitate a nanoparticle, provided it is located well within an optical wavelength from the interface with the material.[4–6]

Of particular interest is the flow pattern of electromagnetic energy in a nano-size system. The simplest and most important source of electromagnetic radiation is the field emitted by an oscillating electric dipole. Already a free dipole can have an interesting radiation pattern in the optical near field. If the dipole moment rotates, as in a $\Delta m = \pm 1$ electronic transition in an atom or as for a microparticle irradiated by a circularly polarized laser beam, the energy emerges from the dipole as a vortex.[7,8] Within a wavelength from the dipole, the field lines of energy flow swirl around the axis through the center of the circle (perpendicular to the plane of rotation), and at larger distances, the field lines become straight, like optical rays. This leads to a shift of the dipole image in the far field due to the rotation near the source.[9] This prediction has been confirmed experimentally.[10]

The simplest substrate is a perfectly conducting mirror. The emission rate of a nearby molecule changes due to the presence of the substrate[11,12] and atomic levels shift due to the nearby metal.[13,14] Also of interest is the behavior of small particles in between two parallel mirrors. Level shifts and altered emission rates have been predicted,[15–23] and suppression of spontaneous emission rates by atoms in between parallel mirrors has been confirmed experimentally.[24–26] The energy flow pattern of dipole radiation

near a mirror has numerous vortices and singularities,[27] and it was found that the vortices are arranged on four optical vortex strings.[28] When the dipole is placed in between parallel mirrors, intricate flow patterns are found,[29] and it is predicted that radiation emerges from the dipole as a set of four vortices.[30]

Here, we shall consider an electric dipole located near the junction of two mirrors, as depicted in Fig. 1. The mirrors meet at a 90° angle, and the coordinate system is as shown. The dipole is located in the *yz* plane, and the mirrors are joint at the *x* axis. This setup was also considered in Ref. 31, where the spontaneous emission rate of an atom in this configuration was computed with a quantum electrodynamical approach.

II. DIPOLE RADIATION

An electric dipole, oscillating at angular frequency ω, has a dipole moment

$$\mathbf{d}(t) = d_o \mathrm{Re}(\hat{\mathbf{u}} e^{-i\omega t}), \quad d_o > 0, \quad \hat{\mathbf{u}}^* \cdot \hat{\mathbf{u}} = 1. \tag{1}$$

If the unit vector $\hat{\mathbf{u}}$ is real, the oscillation is linear. For $\hat{\mathbf{u}}$ complex, the dipole moment vector $\mathbf{d}(t)$ will, in general, trace out an ellipse in a plane. For the complex amplitudes of the emitted and reflected electric and magnetic fields, we shall split off factors as

$$\mathbf{E}(\mathbf{r}) = \zeta \mathbf{e}(\mathbf{r}), \quad \mathbf{B}(\mathbf{r}) = \frac{\zeta}{c}\mathbf{b}(\mathbf{r}), \tag{2}$$

with

$$\zeta = \frac{k_o^3 d_o}{4\pi\varepsilon_o}, \tag{3}$$

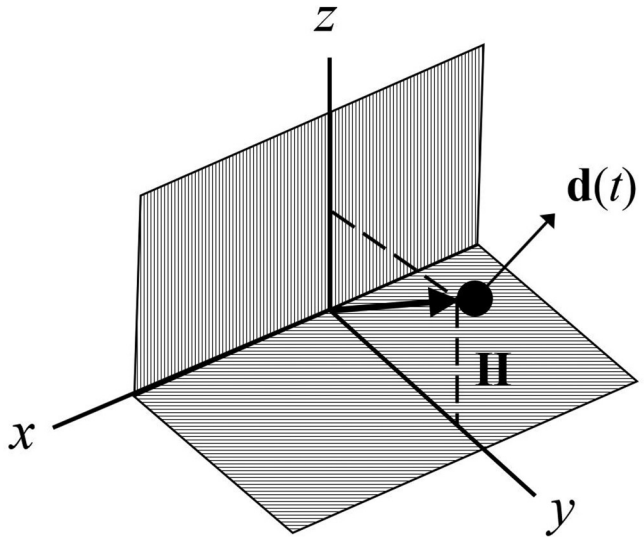

FIG. 1. Shown is the setup of an electric dipole $\mathbf{d}(t)$ located near the junction of two perpendicular mirrors. Vector $\mathbf{H}$ is the position vector of the dipole with respect to the origin of coordinates, and the dipole is located in the *yz* plane. The mirrors have the *x* axis in common.

where $k_o = \omega/c$ is the wavenumber in free space. In this way, $\mathbf{e}(\mathbf{r})$ and $\mathbf{b}(\mathbf{r})$ are dimensionless, and overall constants are accounted for by the single parameter ζ. We also introduce dimensionless coordinates $\bar{x} = k_o x$, $\bar{y} = k_o y$, and $\bar{z} = k_o z$, and in terms of these coordinates, a dimensionless distance of 2π represents an actual distance of an optical wavelength. The complex amplitudes of the electric and magnetic fields are[32]

$$\mathbf{e} = \left\{ \hat{\mathbf{u}} - (\hat{\mathbf{q}} \cdot \hat{\mathbf{u}})\hat{\mathbf{q}} + [\hat{\mathbf{u}} - 3(\hat{\mathbf{q}} \cdot \hat{\mathbf{u}})\hat{\mathbf{q}}] \frac{i}{q}\left(1 + \frac{i}{q}\right) \right\} \frac{e^{iq}}{q}, \tag{4}$$

$$\mathbf{b} = (\hat{\mathbf{q}} \times \hat{\mathbf{u}})\left(1 + \frac{i}{q}\right)\frac{e^{iq}}{q}. \tag{5}$$

Here, $\mathbf{q} = k_o \mathbf{r}$ is the dimensionless position vector of the field point with respect to the location of the dipole, and $q = |\mathbf{q}|$, $\hat{\mathbf{q}} = \mathbf{q}/q$.

III. THE IMAGE SYSTEM

For a dipole near a mirror, some of the emitted radiation reflects at the mirror, and the total field is the sum of the dipole field and the reflected field. The reflected electric and magnetic fields are identical to the fields produced by an image dipole below the mirror. This dipole is located at the same distance below the mirror as the dipole is above the mirror. The dipole moment of the image has its parallel component reversed, as compared to the dipole moment of the source dipole. Hence, if we write $\hat{\mathbf{u}} = \hat{\mathbf{u}}_\perp + \hat{\mathbf{u}}_{||}$ for the dipole moment polarization vector of the source, then $\hat{\mathbf{u}} = \hat{\mathbf{u}}_\perp - \hat{\mathbf{u}}_{||}$ is the dipole moment polarization vector of the image. This is an exact solution of Maxwell's equation and it fully takes retardation into account. The situation is more complicated for the setup with the two mirrors shown in Fig. 1. Let us write $\hat{\mathbf{u}} = (\hat{u}_x, \hat{u}_y, \hat{u}_z)$ for the Cartesian components of the source dipole unit vector and indicate this as $\hat{\mathbf{u}}_1$. Let the image in the *xz* plane be $\hat{\mathbf{u}}_2$. Reversing the parallel component of $\hat{\mathbf{u}}_1$ gives $\hat{\mathbf{u}}_2 = (-\hat{u}_x, \hat{u}_y, -\hat{u}_z)$. But, there is also an image in the *xy* plane $\hat{\mathbf{u}}_4 = (-\hat{u}_x, -\hat{u}_y, \hat{u}_z)$. This image produces a field in the vertical mirror, which needs to be compensated for by the image of $\hat{\mathbf{u}}_4$ in the vertical mirror. This is $\hat{\mathbf{u}}_3 = (\hat{u}_x, -\hat{u}_y, -\hat{u}_z)$. The image system is summarized in Fig. 2. Another way of looking at this is that the two lower dipoles are the images of the two top dipoles, and the two dipoles on the left are the images of the two dipoles on the right.

The electric and magnetic fields of the four dipoles are given by Eqs. (4) and (5), respectively, with the appropriate vector $\hat{\mathbf{u}}$, and vector $\mathbf{q}$ is taken as the position vector of the field point with respect to the particular dipole. When we set $\mathbf{h} = k_o \mathbf{H} = (0, h_y, h_z)$, we have

$$\mathbf{q}_1 = (\bar{x}, \bar{y} - h_y, \bar{z} - h_z), \tag{6}$$

$$\mathbf{q}_2 = (\bar{x}, \bar{y} + h_y, \bar{z} - h_z), \tag{7}$$

$$\mathbf{q}_3 = (\bar{x}, \bar{y} + h_y, \bar{z} + h_z), \tag{8}$$

$$\mathbf{q}_4 = (\bar{x}, \bar{y} - h_y, \bar{z} + h_z), \tag{9}$$

as can be seen from the figure. The total electric and magnetic fields are then the sums of the four individual electric and magnetic fields.

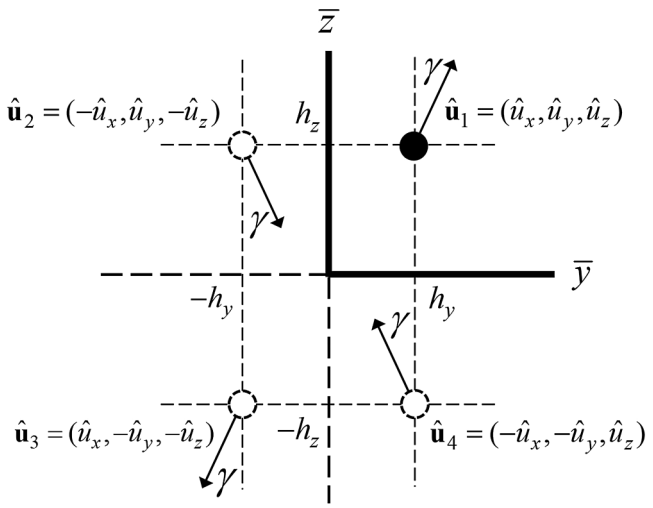

FIG. 2. The figure shows the locations of the image dipoles and their dipole moment polarization vectors. The angles γ shown are for a linear source dipole oscillating in the yz plane, under an angle γ with the positive z axis.

IV. FIELD LINES OF ENERGY FLOW

Electromagnetic energy flows along the field lines of the (time averaged) Poynting vector

$$\mathbf{S}(\mathbf{r}) = \frac{1}{2\mu_o}\mathrm{Re}[\mathbf{E}(\mathbf{r})^* \times \mathbf{B}(\mathbf{r})]. \tag{10}$$

We introduce the dimensionless Poynting vector $\boldsymbol{\sigma} = 2\mu_o c\mathbf{S}/\zeta^2$ so that

$$\boldsymbol{\sigma} = \mathrm{Re}(\mathbf{e}^* \times \mathbf{b}), \tag{11}$$

which is now considered a function of the dimensionless field point coordinates $(\bar{x}, \bar{y}, \bar{z})$, or equivalently, a function of $\mathbf{q}$. We parametrize a field line of the vector field $\boldsymbol{\sigma}$ by $\mathbf{q}(u)$, with u being a dummy variable. The $\bar{x}$ coordinate of a point on the field line through a given point $(\bar{x}_o, \bar{y}_o, \bar{z}_o)$ is then the solution of

$$\frac{d}{du}\bar{x}(u) = \sigma_x(\bar{x}(u), \bar{y}(u), \bar{z}(u)), \tag{12}$$

and similar equations hold for the $\bar{y}$ and $\bar{z}$ coordinates. This set of three equations can be solved numerically for a given initial point $(\bar{x}_o, \bar{y}_o, \bar{z}_o)$. The field lines run into the direction of increasing u. Near the dipole, the fields $\mathbf{e}_1$ and $\mathbf{b}_1$ (fields of the source dipole) diverge, which may give numerical problems. Field lines are only determined by the directions of the vectors of the vector field, so if we multiply $\boldsymbol{\sigma}$ by any positive function f of $\bar{x}$, $\bar{y}$, and $\bar{z}$, the field lines remain the same. A good choice seems to be $f = q_1^5$.

Due to boundary conditions, near the surface of a mirror, the electric field is perpendicular to the mirror surface, and the magnetic field is parallel to the surface. Therefore, near a mirror, a field line of energy flow is parallel to the mirror surface. This should be so because energy cannot penetrate a perfectly conducting material.

V. DIPOLE AND FIELD LINES IN THE *YZ* PLANE

In this section, we shall consider a dipole oscillating or rotating in the yz plane so that $\hat{u}_x = 0$. It can then be checked from Eqs. (4) and (5) that, for a field point in the yz plane, the electric field is in the yz plane, and the magnetic field only has an x component. The corresponding Poynting vector at such a point is then in the yz plane. Therefore, if a field line goes through a point in the yz plane, it stays in the yz plane. The field lines are 2D curves, whereas, in general, they will be 3D curves. For a linear dipole, we set

$$\hat{\mathbf{u}} = (0, \sin\gamma, \cos\gamma), \tag{13}$$

so this corresponds to a dipole oscillating back and forth along vector $\hat{\mathbf{u}}$, which makes an angle γ with the positive z axis.

A typical energy flow pattern is shown in Fig. 3, where $\gamma = \pi/3$, $h_y = 10$, and $h_z = 5$. The field lines start at the location of the dipole. Far away from the dipole and the mirrors, field lines become straight. Near the intersection corner of the mirrors, the field lines need to bend so that they become parallel to the mirror surfaces. This leads to an intricate flow pattern with singularities and optical vortices. Figure 4 shows an enlargement of the flow pattern near the corner. The black circle is the center of the vortex, and the two white circles are singularities where field lines split. Figure 5 shows an enlargement of the flow lines in the neighborhood of the dipole. There are two vortices and three other singularities. Interestingly,

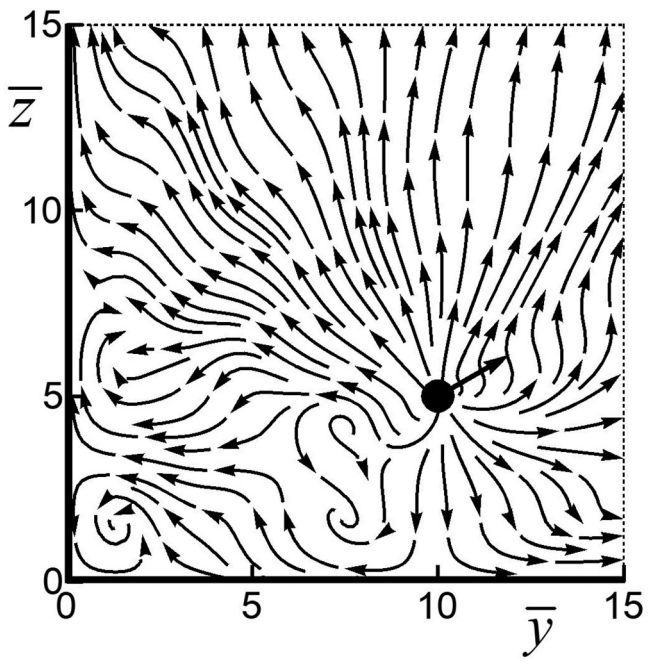

FIG. 3. Shown is the energy flow pattern for a linear dipole, oscillating under 60° with the z axis.

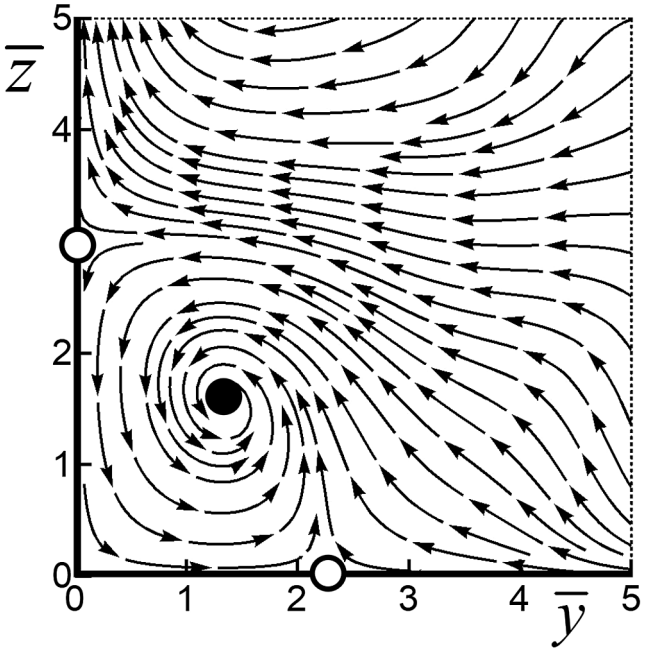

FIG. 4. The figure shows an enlargement of the vortex in the lower-left corner in Fig. 3.

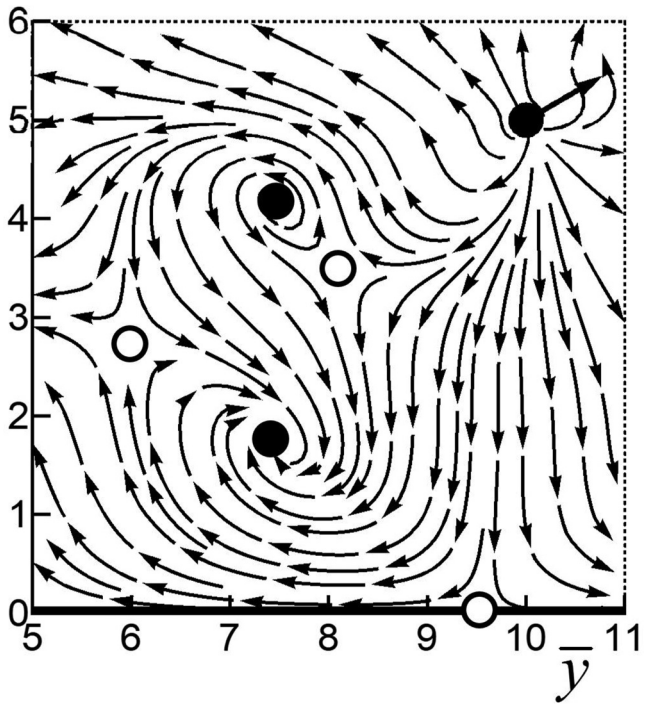

FIG. 5. The figure shows an enlargement near the dipole of the flow line pattern in Fig. 3.

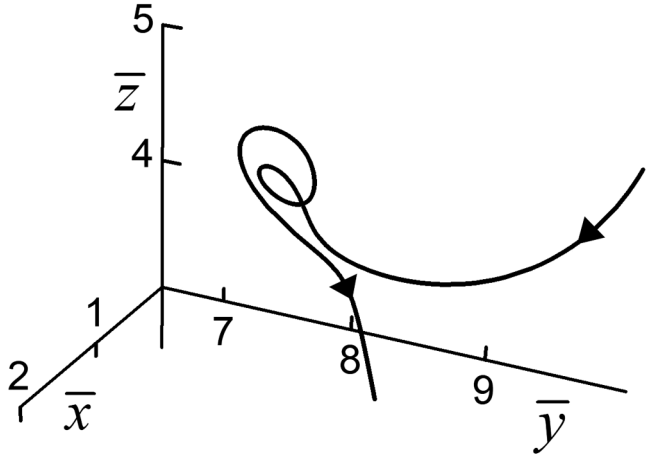

FIG. 6. Shown is a 3D field line near the top vortex in Fig. 5.

there are field lines that seem to start at the center of the upper vortex and end at the center of the lower vortex. Clearly, energy cannot be created at the center of the top vortex, and then accumulate at the lower vortex. The divergence of the Poynting vector is zero, so the field has no sources and sinks outside the dipole. All energy comes out of the dipole and eventually flows away to infinity. The explanation of this phenomenon is illustrated in Fig. 6. Figure 6 shows a 3D field line near the top vortex. The dipole is just outside the picture, located at (0, 10, 5). The incoming field line is well off the yz plane. Near the center of the vortex in the yz plane, it swirls around and then it leaves. The outgoing branch stays very close to the yz plane, although that cannot be seen directly from the graph. Field lines cannot cross, so, in particular, the field line shown in the figure cannot cross the yz plane.

In Fig. 7, the dipole is symmetrically placed with respect to the mirrors, and it oscillates under an angle of $\pi/4$ with the positive z axis. The 45° line is a singular line, and it can be shown that this is due to the vanishing of the magnetic field. Field lines come out of the dipole, bend to the dipole axis, and then stop at the diagonal line. In this figure, the dipole is located at $h_y = h_z = 1.5$. If we increase the distance to the origin by taking $h_y = h_z = 4$, then the field lines start at the diagonal singular line in the region above the dipole but still end on the singular line in the region between the dipole and the mirror. If we increase the distance further to $h_y = h_z = 6$, two vortices appear in the region between the dipole and the mirrors. This is shown in Fig. 8. When the dipole is close to the mirrors, some field lines that come out of the dipole return to the dipole at the other side. These closed loop field lines are shown in Fig. 9.

VI. LOCATIONS OF VORTICES AND SINGULARITIES

The energy flow field line pattern is mainly determined by the vortices and singularities in the field of the Poynting vector. At the center of a vortex or any other singularity, the Poynting vector vanishes, leaving the direction of $\boldsymbol{\sigma}$ undetermined. At the center of a

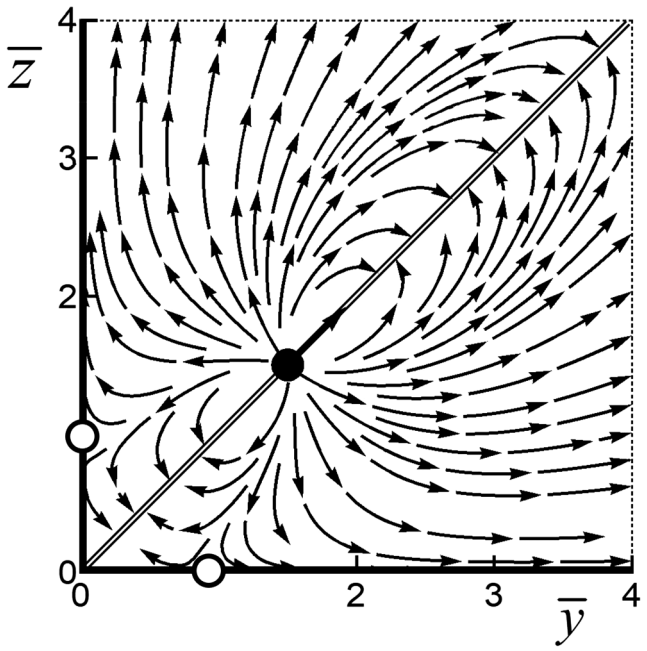

FIG. 7. Shown is the energy flow diagram for a dipole oscillating under 45° with the z axis and symmetrically placed with respect to the mirrors.

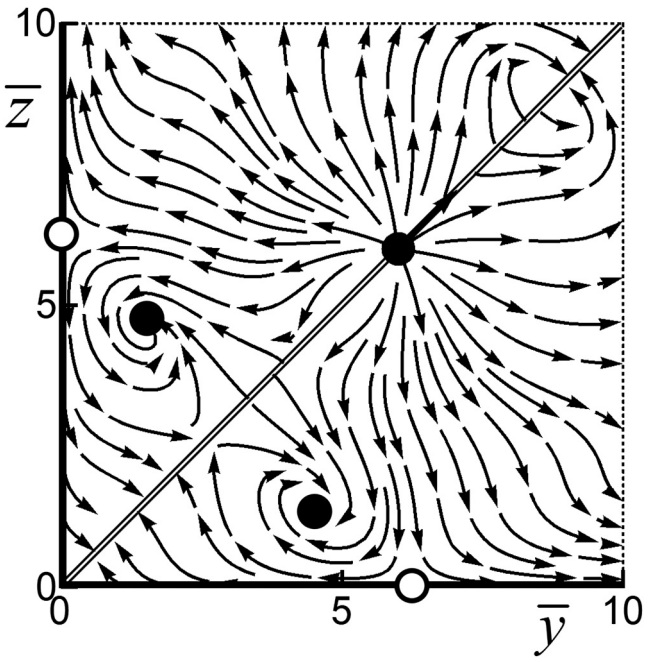

FIG. 8. The same dipole of Fig. 7 is now further away from the origin of coordinates, and two vortices appear.

vortex, the magnetic field vanishes.[27] In the yz plane, the complex amplitude of the magnetic field is along the x axis, so for $\mathbf{b}$ to vanish, both the real parts and the imaginary part of b_x have to be zero at the same point in the yz plane. We solve $\mathrm{Re}b_x = 0$ and $\mathrm{Im}b_x = 0$ numerically. The solution of each equation can be represented by a set of curves in the yz plane. We use solid curves for the solutions of $\mathrm{Re}b_x = 0$ and dashed curves for the solutions of $\mathrm{Im}b_x = 0$. At the intersection of a solid curve and a dashed curve, the magnetic field is zero, and this indicates the center of a vortex. Figure 10 shows the solutions of $\mathrm{Re}b_x = 0$ and $\mathrm{Im}b_x = 0$ for the field line pattern in Fig. 5, so for $\gamma = \pi/3$, $h_y = 10$, and $h_z = 5$. The two black circles indeed correspond to the locations of the two vortices in Fig. 5.

At any singularity, $\boldsymbol{\sigma} = 0$. Since $\boldsymbol{\sigma}$ is in the yz plane and real, we set $\sigma_y = 0$ and $\sigma_z = 0$ to find all singularities. The solutions of $\sigma_y = 0$ are represented by sets of solid curves, and the solutions of $\sigma_z = 0$ are indicated by dashed curves. At any intersection between a solid curve and a dashed curve, we must have a singularity. Figure 11 shows the singularities for the flow lines in Fig. 5. In the middle of the graph are four singularities, and comparison with Fig. 10 then tells us which singularities are centers of vortices (black circles) and which are other singularities (white circles). At these other singularities, we have points where field lines split, and it can be shown that at these points $\mathbf{e}^* \times \mathbf{b}$ is imaginary. On the z axis, the Poynting vector is necessarily along the z axis, so the z axis is a solid curve. Similarly, the y axis is a dashed curve. In Fig. 11, the solid curve coming down from the dipole hits the y axis, so this curve ends at a singularity on the y axis. We see from

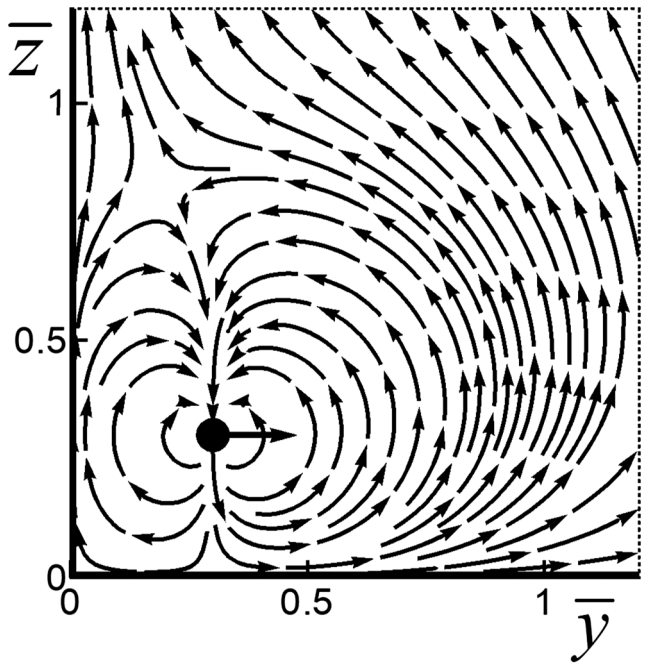

FIG. 9. The dipole oscillates horizontally and is close to the corner. Field lines come out of the dipole at the bottom, and some return the dipole at the top. These are closed loops of energy flow.

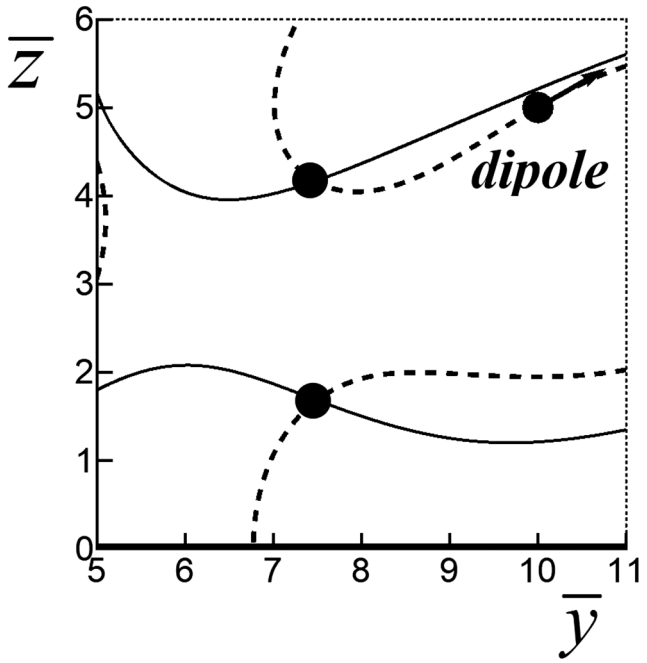

FIG. 10. The intersections between a solid curve and a dashed curve are points where the magnetic field vanishes, and these are the singular points at the centers of vortices.

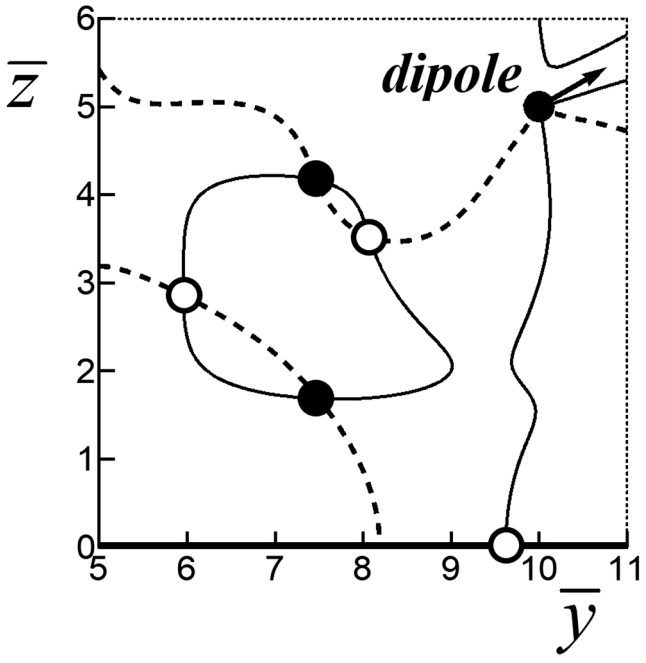

FIG. 11. The intersections between a solid curve and a dashed curve are points where the Poynting vector vanishes, and these are the singular points of the flow line pattern.

Fig. 5 that this is indeed a point where field lines split at the mirror surface.

Most of the vortices and singularities appear in the area between the dipole and the corner of the two mirrors. Such flow patterns can be very complicated, and field line graphs are sometimes not able to show sufficient detail, unless enlargements are made, as in Fig. 4. We consider again a dipole located at $h_y = 10$, $h_z = 5$, but now we take

$$\hat{\mathbf{u}} = \frac{1}{\sqrt{2}}(0, 1, i). \tag{14}$$

This is a dipole moment, rotating counterclockwise in the yz plane. Figure 12 shows the locations of the vortices, and Fig. 13 shows all singularities. Clearly, without considering the locations of the vortices first with Fig. 12, we could never have been able to determine the nature of the singularities in Fig. 13.

VII. FIELD LINES IN THE PLANE OF THE HORIZONTAL MIRROR

We now consider field lines of the Poynting vector in the xy plane. This vector is parallel to the surface at any point in the xy plane, so the field lines are 2D curves in the xy plane for any state of oscillation $\hat{\mathbf{u}}$ of the dipole moment. A typical example is shown in Fig. 14. As compared to the view in Fig. 1, we now have the joint x axes to the right, so we look "over the edge, from the left" in

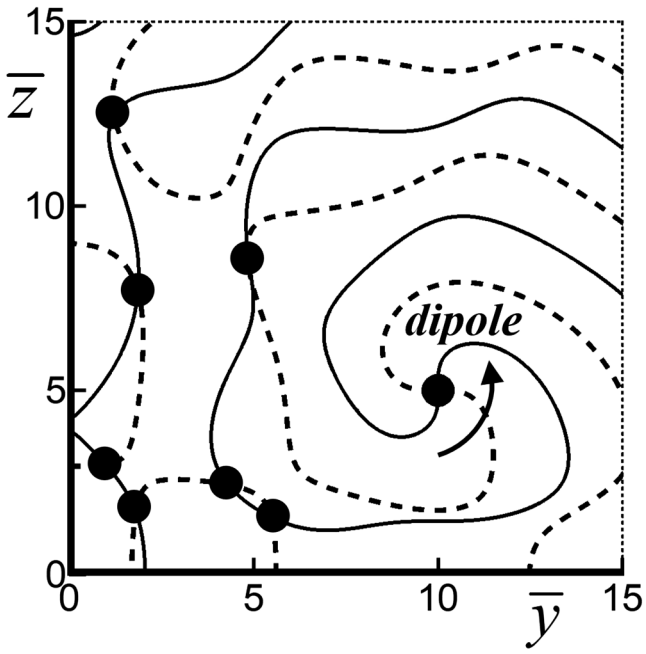

FIG. 12. Shown are the locations of vortices for a rotating dipole moment.

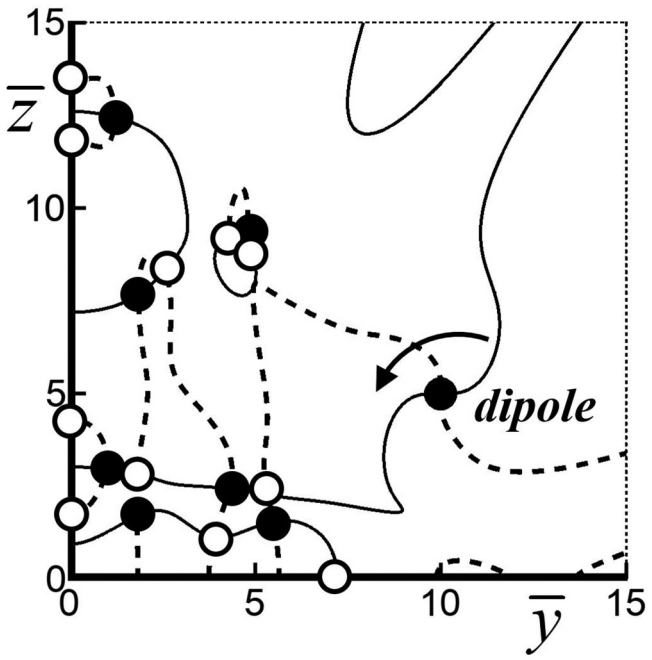

FIG. 13. Shown are the locations of singularities for a rotating dipole moment.

Fig. 1. The dashed white circle is the projection of the dipole onto the xy plane. For Fig. 14, we have $h_y = 3$, $h_z = 1$, and the dipole moment rotates counterclockwise in the xy plane.

The dark line at the bottom of the figure is the x axis, so the second mirror is perpendicular to this and upwards. It seems that field lines are coming out of the x axis on the left and end on the x axis on the right. In the Appendix, explicit expressions for the electric and magnetic field amplitudes for a field point in the xy plane are given. When we set $y = 0$, we have $q_2 = q_1$, and with Eq. (A1) this gives $\mathbf{e} = 0$, and, therefore, $\boldsymbol{\sigma} = 0$. The x axis is a singular line and field lines can end or start there. The magnetic field on the x axis is

$$\mathbf{b} = 4\mathbf{e}_x(h_z\hat{u}_y - h_y\hat{u}_z)\left(1 + \frac{i}{q_1}\right)\frac{e^{iq_1}}{q_1^2}, \tag{15}$$

which is along the x axis. We can also see this as follows. At the surface of a perfect conductor, $\mathbf{e}$ has to be perpendicular to the surface. The mirrors are joint at the x axis, so $\mathbf{e}$ has to be perpendicular to both surfaces. This is only possible if $\mathbf{e}$ is zero. Similarly, $\mathbf{b}$ has to be parallel to the surface of a perfect conductor. At the junction, this is only possible if $\mathbf{b}$ is along the x axis. From $\mathbf{e} = 0$, we have $\boldsymbol{\sigma} = 0$, no matter what $\mathbf{b}$ is.

Just like for field lines in the yz plane, we can here draw curves with $\sigma_x = 0$ (solid lines) and $\sigma_y = 0$ (dashed lines). An example is shown in Fig. 15, where $\gamma = \pi/3$, $h_y = 5$, and $h_z = 3$. Since the dipole oscillates in the yz plane, the figure is symmetric between left and right. Here, we have the peculiar situation that on the top part of the Ω-shaped figure the solid and dashed lines coincide. Therefore, this part is a singular curve, and it can be seen that

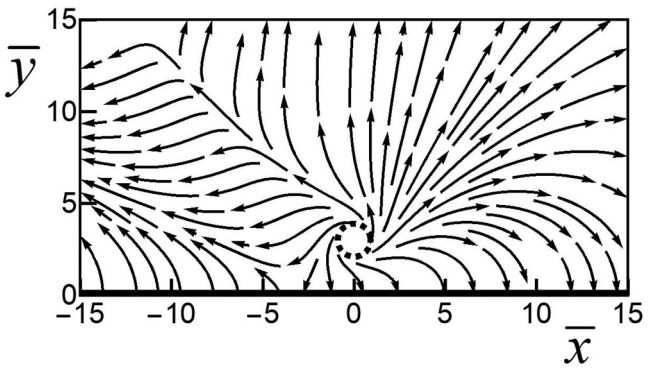

FIG. 14. The figure shows field lines of the Poynting vector for a dipole moment, rotating in the xy plane.

the field lines change their direction across this curve. On the lower part of the Ω-shaped figure, the solid and dashed lines separate, and the field lines cross the solid curves vertically (hard to see in the figure) and they cross the dashed curves horizontally. Since the magnetic field is not zero on the Ω-shaped curve, these are singularities where $\mathbf{e}^* \times \mathbf{b}$ is imaginary. There is both an electric field and a magnetic field, but $\mathbf{e}^*$ and $\mathbf{b}$ are out of phase, just so as to make the Poynting vector zero.

Another interesting case is shown in Fig. 16. Here, we have $\gamma = \pi/2$, so the dipole oscillates horizontally in the yz plane, parallel to the lower mirror. We have $h_y = h_z = 10$. It can be shown from Eq. (A1) that $\mathbf{e}$ is along the z axis, $\mathbf{b}$ is along the x axis, and therefore the Poynting vector is along the y axis everywhere. We have $\sigma_x = 0$ everywhere, and so the "solid line" is the entire mirror surface. Consequently, all points on a dashed curve do not only have $\sigma_y = 0$, but also $\sigma_x = 0$. Therefore, the dashed curves are singular curves, and we see from the figure that the field lines change their direction across these curves.

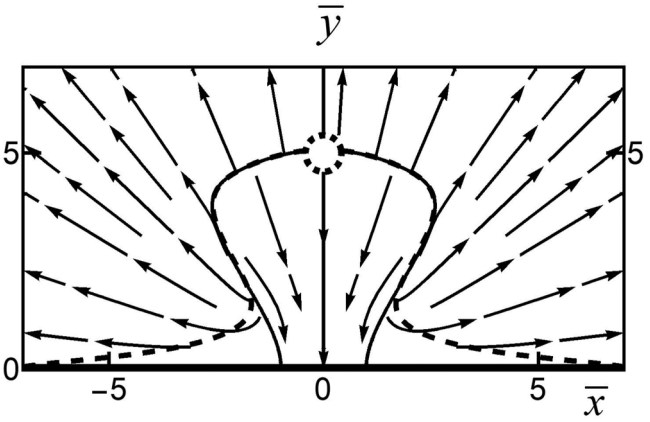

FIG. 15. The figure shows field lines of the Poynting vector in the xy plane for a dipole oscillating in the yz plane, under an angle of 60° with the z axis.

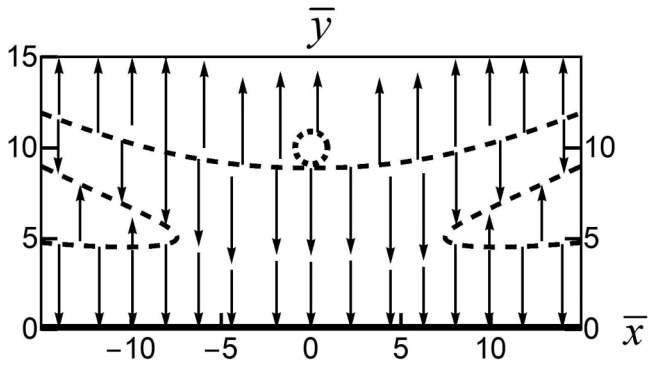

FIG. 16. Shown are field lines of the Poynting vector in the *xy* plane for a dipole oscillating parallel to the horizontal mirror and perpendicular to the vertical mirror.

VII. CURRENT DENSITY IN THE MIRRORS

The magnetic field induces a surface current density in the horizontal mirror according to

$$\mathbf{i}(\mathbf{r}, t) = \frac{1}{\mu_o}\mathbf{e}_z \times \mathbf{B}(\mathbf{r}, t), \tag{16}$$

with $\mathbf{B}(\mathbf{r}, t)$ being the magnetic field just above the surface. Unlike the time-averaged Poynting vector, the current density varies with time, and its time average is zero. We define the dimensionless current density $\mathbf{I}(\mathbf{r}, t) = \mathbf{i}(\mathbf{r}, t)/i_o$, with $i_o = \zeta/(\mu_o c)$. We then have

$$\mathbf{I}(\mathbf{r}, t) = \mathrm{Re}[\mathbf{e}_z \times \mathbf{b}(\mathbf{r})e^{-i\omega t}]. \tag{17}$$

The field $\mathbf{b}$ at the surface is given by Eq. (A2), and we obtain immediately

$$\mathbf{I}(\mathbf{r}, t) = \frac{2}{q_1^2}\mathrm{Re}\left[(\mathbf{q}_{1,||}\hat{u}_z + h_z\hat{\mathbf{u}}_{||})\left(1 + \frac{i}{q_1}\right)e^{i(q_1 - \bar{t})}\right] - \frac{2}{q_2^2}\mathrm{Re}\left[(\mathbf{q}_{1,||}\hat{u}_z + h_z\hat{\mathbf{u}}_{||} + 2(h_y\hat{u}_z - h_z\hat{u}_y)\mathbf{e}_y)\left(1 + \frac{i}{q_2}\right)e^{i(q_2 - \bar{t})}\right], \tag{18}$$

which is now a function of $\bar{x}$, $\bar{y}$ and the dimensionless time variable $\bar{t} = \omega t$. In the figures, we shall draw solid lines for the solutions of $I_x = 0$ and dashed lines for the solutions of $I_y = 0$.

As a first example, we set $\hat{\mathbf{u}} = \mathbf{e}_x$. Equation (18) then simplifies to

$$\mathbf{I}(\mathbf{r}, t) = 2h_z\mathbf{e}_x\left\{\frac{1}{q_1^2}\left[\cos(q_1 - \bar{t}) - \frac{1}{q_1}\sin(q_1 - \bar{t})\right] - \frac{1}{q_2^2}\left[\cos(q_2 - \bar{t}) - \frac{1}{q_2}\sin(q_2 - \bar{t})\right]\right\}. \tag{19}$$

The current density is in the positive or negative x direction, and the field line diagram is shown in Fig. 17 for $t = 0$. Also shown are the solid lines, representing $I_x = 0$. These are singular curves of the field line pattern, and we see that the current density changes its direction across a singular curve. For a point on the x axis, we have $q_1 = q_2$, and we see from Eq. (19) that this gives $\mathbf{I} = 0$. Therefore, the x axis is a singular line.

When t increases, the current density vector $\mathbf{I}(\mathbf{r}, t)$ oscillates back and forth in the x direction at a given field point $\mathbf{r}$. This means that the singular curves $I_x = 0$ in Fig. 17 change their shape when time passes. Field lines run from one curve to the next one, and the directions alternate across each curve. So, if we can find how the curves move with time, then the field lines just stay between the moving curves as in Fig. 17. We shall consider the curves at field points with $\bar{y} \gg 1$, so at least several wavelengths away from the vertical mirror. We also assume $\bar{y} \gg h$, so the field point is at least several wavelengths away from the location of the dipole. This corresponds to the top part of the pattern in Fig. 17. From Eq. (6), we have

$$q_1 = \sqrt{\bar{\rho}^2 + h^2 - 2h_y\bar{y}}, \tag{20}$$

with $\bar{\rho} = (\bar{x}^2 + \bar{y}^2)^{1/2}$ as the dimensionless distance to the origin. Far away this becomes

$$q_1 \approx \bar{\rho} - h_y\frac{\bar{y}}{\bar{\rho}}, \tag{21}$$

and in the same way, we find

$$q_2 \approx \bar{\rho} + h_y\frac{\bar{y}}{\bar{\rho}}. \tag{22}$$

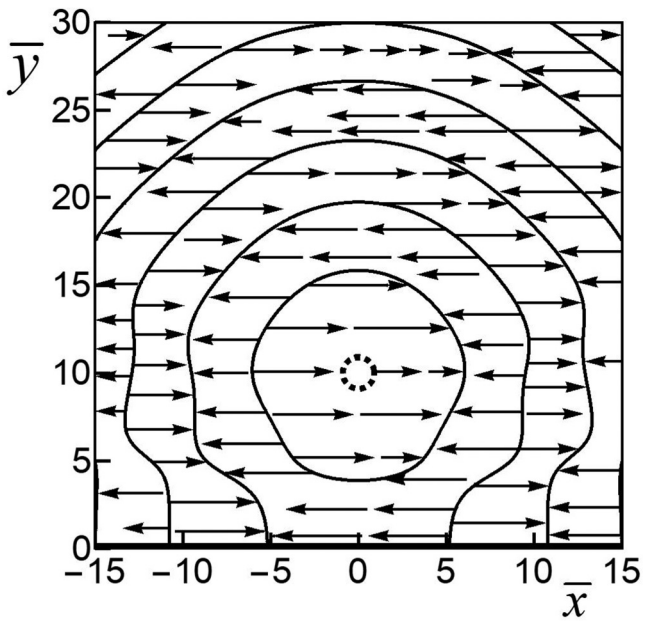

FIG. 17. The figure shows field lines of the current density in the horizontal mirror at $t = 0$ for a dipole oscillating along the x direction. The dipole is located at (0, 10, 5).

This gives for the current density

$$\mathbf{I}(\mathbf{r}, t) \approx \frac{4h_z}{\bar{\rho}^2}\mathbf{e}_x \sin\left(h_y \frac{\bar{y}}{\bar{\rho}}\right)\left[\sin(\bar{\rho}-\bar{t}) + \frac{1}{\bar{\rho}}\cos(\bar{\rho}-\bar{t})\right]. \tag{23}$$

For a singular curve, the term in square brackets vanishes. This term only depends on $\bar{\rho}$, for a given $\bar{t}$. If we set $\bar{\rho} = \bar{R}$ for a solution, then the corresponding singular curve is a semi-circle with dimensionless radius $\bar{R}$. So, these radii are solutions of

$$\cot(\bar{R}-\bar{t}) = -\bar{R}, \tag{24}$$

and this makes $\bar{R}$ a function of $\bar{t}$. When we differentiate Eq. (24) with respect to $\bar{t}$, we obtain

$$\frac{d\bar{R}}{d\bar{t}} = 1 + \frac{1}{\bar{R}^2}. \tag{25}$$

The left-hand side is the rate of increase of $\bar{R}$, so this is the dimensionless speed at which this $\bar{R}$ grows. This is the radial speed at which the corresponding circle expands. We can see this as a current density wave on the xy plane so that this speed is the phase velocity of the expanding wave. Going back to real variables (rather than dimensionless variables) then gives for the phase velocity of the expanding waves

$$v_{ph} = \left(1 + \frac{1}{\bar{R}^2}\right)c, \tag{26}$$

with c being the speed of light. Clearly, the phase velocity is larger than the speed of light, and for large $\bar{R}$, it approaches the speed of light. This means that circles with a small radius move faster than circles far away. This can be understood from Eq. (24). When we graph the left-hand side and the right-hand side as a function of $\bar{R}$, the solutions are at the intersections of the two graphs. For large $\bar{R}$, the intersections are as good as at the locations of the asymptotes of the cotangent, so the solutions are approximately $\bar{R} = n\pi$. At smaller distances, the values of $\bar{R}$ are somewhat smaller, and so the spacing between the solutions is bigger. Therefore, a wave front (singular curve) with smaller $\bar{R}$ has to cover more distance in the same time than a wave front with large $\bar{R}$, and, therefore, it must have a larger phase velocity. This also shows that the singular curves are approximately π apart, and this is half an optical wavelength.

Equation (15) gives the complex amplitude of the magnetic field on the x axis. With Eq. (17), we then find for the current density on the x axis,

$$\mathbf{I}(\mathbf{r}, t) = \mathbf{e}_y \frac{4}{q_1^2}\mathrm{Re}\left[(h_z\hat{u}_y - h_y\hat{u}_z)\left(1 + \frac{i}{q_1}\right)e^{iq_1}\right], \tag{27}$$

and we see that it is in the positive or negative y direction. Therefore, the current density flows toward the intersection of the mirrors or away from it, and under 90°. The current density is only zero on the x axis if $\hat{\mathbf{u}} = \mathbf{e}_x$, as in the example above. Figure 18 shows the field lines of the current density for $\gamma = 60^\circ$ at $t = 0$.

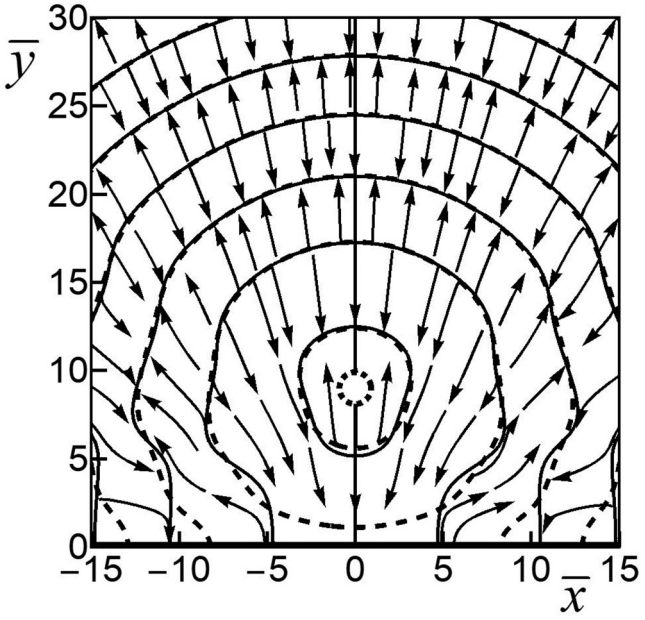

FIG. 18. Shown are field lines of the current density in the horizontal mirror for $\gamma = \pi/3$ and $t = 0$. The dipole is located at (0, 9, 7).

When time progresses, the singular curves expand, similar to the case of the linear dipole along the x axis. At some locations on the x axis, the current flows toward the x axis, and at other places, it flows away from it. Due to the scale of the figure, it cannot be seen what happens in the neighborhood of $x = 0$. An enlargement is shown in Fig. 19, and we see that, in this region, the current flows in the positive y direction. Obviously, current cannot be created at the x axis, and the only possibility is that it flows toward the xy plane along the vertical mirror. For the current density in the vertical mirror, just above the x axis, we find

$$\mathbf{I}(\mathbf{r}, t) = -\mathbf{e}_z \frac{4}{q_1^2}\mathrm{Re}\left[(h_z\hat{u}_y - h_y\hat{u}_z)\left(1 + \frac{i}{q_1}\right)e^{iq_1}\right]. \tag{28}$$

Here, the term in square brackets is the same as in Eq. (27), so when the current from Eq. (27) flows away from the x axis, then the current from Eq. (28) flows toward the x axis. The current flowing down the vertical mirror hits the x axis under 90°. Then, it makes a 90° turn and continues flowing away in the xy plane, initially under 90°. Figure 20 shows the current density in the xz plane for the same parameters as in Figs. 18 and 19. The view here is that x goes to the right, and z goes up, so we look at the vertical mirror from behind, which is from the left in Fig. 1.

Finally, we consider a dipole moment rotating in the xy plane. For such a dipole, the polarization vector is $\hat{\mathbf{u}} = (1, i, 0)/\sqrt{2}$. The current density in the xy plane is shown in Fig. 21, where we took the dipole to be located at (0,10,5). There are no singularities or vortices for this case. A close inspection of the graph shows that

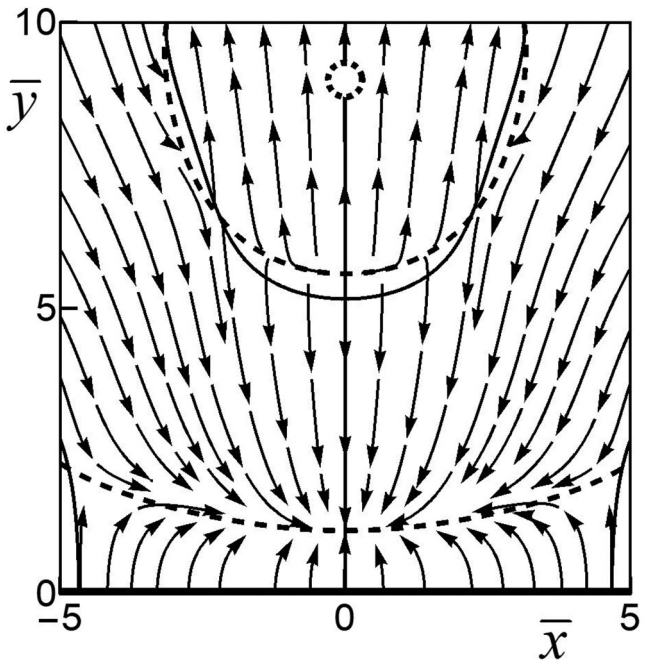

FIG. 19. The figure shows an enlargement of a part of the graph in Fig. 18.

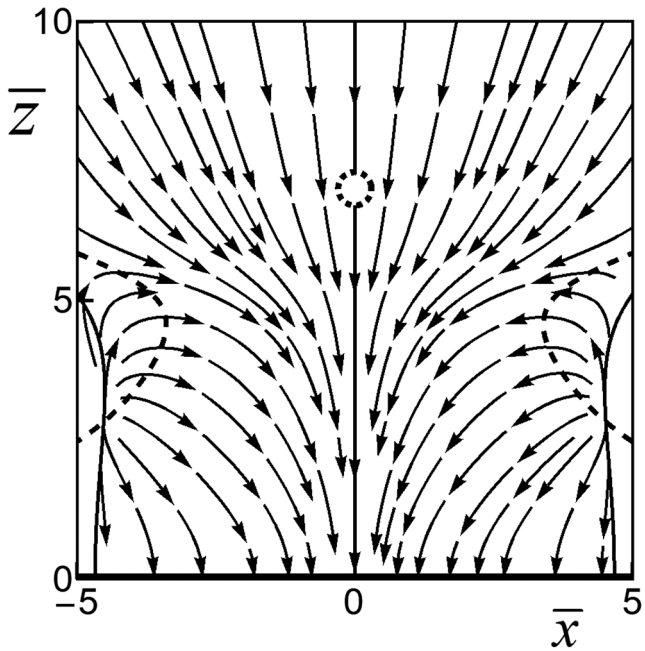

FIG. 20. Shown are field lines of the current density in the vertical mirror. At the bottom part of the picture, the current flows toward the *x* axis. There, it makes a 90° turn toward the positive *y* direction, and it continues flowing in the *xy* plane, as shown in Fig. 19.

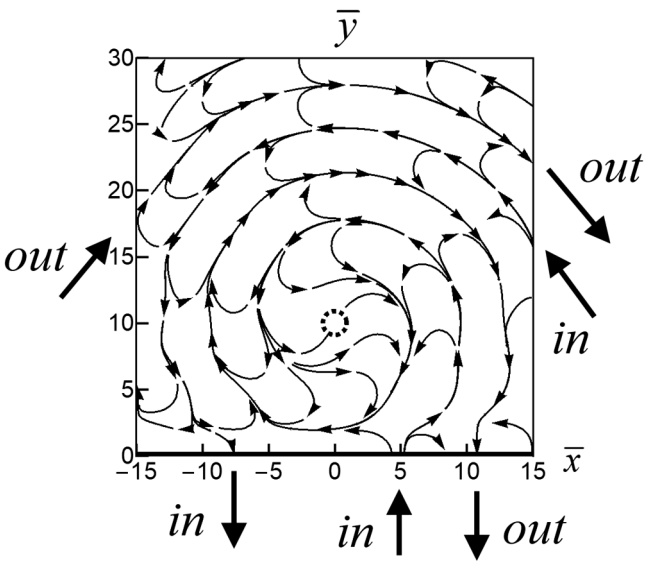

FIG. 21. Field lines of the current density in the horizontal mirror for a dipole moment rotating in the *xy* plane.

the circular-looking curves are not closed loops. They actually form an infinite spiral. Starting from *in* on the right-hand side of the picture, the spiral is incoming and spirals counterclockwise. At *in* on the left on the bottom, the spiral runs outside the picture

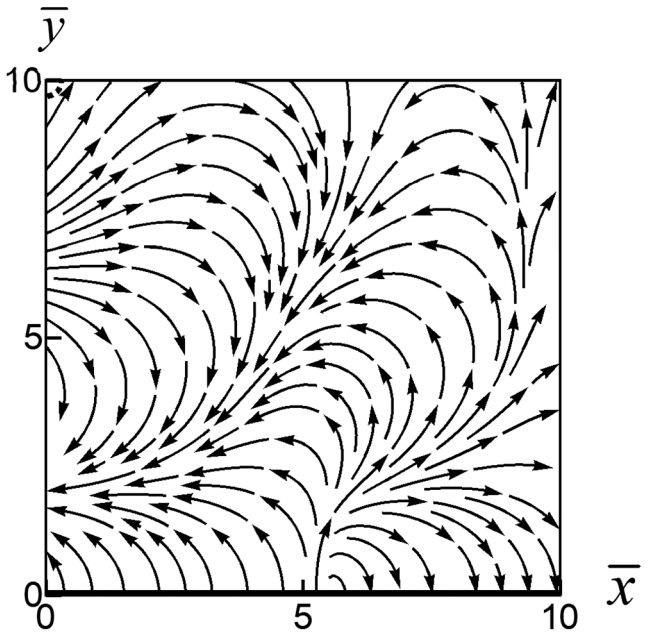

FIG. 22. The figure shows an enlargement of a part of the flow line pattern of Fig. 21. The dipole is just in the top-left corner.

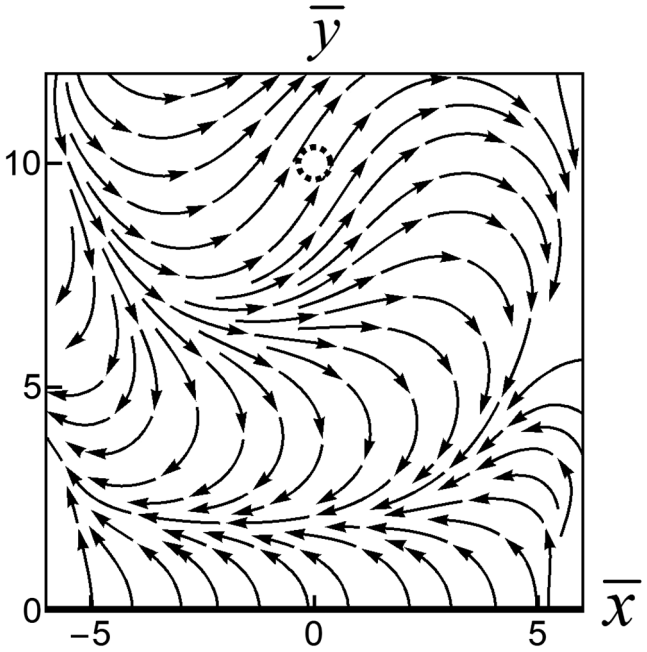

FIG. 23. Shown is an enlargement of a part of Fig. 21, in the neighborhood of the dipole. The field lines going down in the top-left of the figure form the end of the incoming spiral. At the dipole, they continue as the beginning of the outgoing spiral, running to the left under the dipole in the lower part of the diagram.

and returns near $\bar{x} = 5$ on the right. The curve spirals in until it passes through the projection of the dipole (dashed circle), and then it reverses its direction to a clockwise rotation. At *out* near $\bar{x} = 10$ it leaves the picture and then it continues inside the view to *out* on the left. Finally, it leaves the picture at *out* on the right. The clockwise outgoing spiral runs in between the counterclockwise incoming spiral, and as such the whole picture is one curve, except that near the vertical mirror on the x axis we imagine that it "continues" outside the horizontal mirror. All field lines of the current density come in approximately over the incoming spiral. At some point along the incoming spiral, a field line makes turn, either left or right, and catches up with the outgoing spiral. Then, the field line continues spiraling outward along this outgoing spiral. An enlargement of this splitting along the spiral in left and right going field lines is shown in Fig. 22, and Fig. 23 shows an enlargement of the transition from incoming to outgoing at the location of the dipole.

VII. CONCLUSIONS

We have considered an oscillating electric dipole near the corner of two orthogonal mirrors, as depicted in Fig. 1. The electric and magnetic fields in the space between the mirrors are identical to the fields by the dipole and three mirror images, as shown in Fig. 2. We have studied the field lines of energy flow in the yz plane for a dipole moment oscillating or rotating in the yz plane. The field lines have very intricate structures, depending on the state of oscillation of the dipole and the distances to each of the mirrors. Numerous vortices and singularities appear. It was shown that field lines that seem to end at the center of a vortex are part of a 3D bundle of field lines that approach the dipole and then swirl away after passing near the center of the vortex. The flow line patterns are largely determined by the presence of singularities and vortices in the flow field. We have shown that the locations of vortices can be found by solving for the points where the magnetic field complex amplitude vanishes. On solid curves in the figures, the real part of the magnetic field amplitude vanishes, and on dashed curves, the imaginary part is zero. Any intersection of a solid curve with a dashed curve then signifies the location of a vortex. Similarly, by considering curves where the y (solid curves) and z (dashed curves) components of the Poynting vector are zero, any intersection of a solid curve and a dashed curve represents a singularity. By comparison with a graph showing where the magnetic field vanishes for the same parameters, we know which intersections indicate centers of vortices. The remaining singularities are points in the flow pattern where field lines split in different directions or where field lines end.

The dipole and its images induce a surface current density in the mirrors. Equation (18) gives an explicit expression for this current density in the horizontal mirror (xy plane). We now draw curves in the current flow diagrams where the x component (solid curves) or the y component (dashed curves) of the surface current density is zero. At an intersection between a solid curve and a dashed curve, we have a singularity on the flow diagram. We see in Fig. 18 that the dashed and solid curves are as good as identical, except close to the vertical mirror. For a linear dipole, field lines run approximately radially outward or inward, and a field line changes direction every time it crosses a singular curve. It was shown that the singular curves expand with time, with a phase velocity greater than the speed of light. In between singular curves, the current density keeps its direction (inward or outward), so the entire picture expands rapidly, with new singular curves being produced at the location of the projection of the dipole onto the xy plane. Current flowing to the intersection of the mirrors hits the intersection line under 90°, and it continues to flow in the vertical mirror.

For a dipole moment rotating in the xy plane, the current density also changes direction across curves, but these are not singular curves, and they are not closed curves. Field lines come in along an in-spiraling curve, and then suddenly deviate to the left or the right. They catch up with another arm of the same spiral, and this part of the spiral runs outward, in between the curves of the incoming part of the spiral. The spiral expands in time with a phase velocity larger than the speed of light, and the current flow field line pattern expands with it.

APPENDIX: FIELDS IN THE *xy* PLANE

The complex amplitude of the electric field of each of the four dipoles is given by Eq. (4), with $\mathbf{q}$'s given by Eqs. (6)–(9) and $\hat{\mathbf{u}}$'s are shown in Fig. 2. The total field is the sum of the four. For a field point in the xy plane, we have $q_4 = q_1$ and $q_3 = q_2$, and with some manipulations we find

$$\mathbf{e} = 2\mathbf{e}_z\left\{\hat{u}_z + \frac{1}{q_1^2}(\mathbf{q}_1\cdot\hat{\mathbf{u}})h_z + \left[\hat{u}_z + \frac{3}{q_1^2}(\mathbf{q}_1\cdot\hat{\mathbf{u}})h_z\right]\frac{i}{q_1}\left(1+\frac{i}{q_1}\right)\right\}\frac{e^{iq_1}}{q_1}$$
$$- 2\mathbf{e}_z\left\{\hat{u}_z + \frac{1}{q_2^2}(\mathbf{q}_1\cdot\hat{\mathbf{u}} - 2\hat{y}\hat{u}_y)h_z + \left[\hat{u}_z + \frac{3}{q_2^2}(\mathbf{q}_1\cdot\hat{\mathbf{u}} - 2\bar{y}\hat{u}_y)h_z\right]\frac{i}{q_2}\left(1+\frac{i}{q_2}\right)\right\}\frac{e^{iq_2}}{q_2}. \quad \text{(A1)}$$

Here, the reference to the image dipoles has disappeared, except that the distance q_2 is still there. The electric field complex amplitude is in the z direction, so perpendicular to the surface, as it should be. For the magnetic field complex amplitude, we find

$$\mathbf{b} = -\frac{2}{q_1^2}\mathbf{e}_z\times(\mathbf{q}_{1,||}\hat{u}_z + h_z\hat{\mathbf{u}}_{||})\left(1+\frac{i}{q_1}\right)e^{iq_1}$$
$$+\frac{2}{q_2^2}\mathbf{e}_z\times(\mathbf{q}_{1,||}\hat{u}_z + h_z\hat{\mathbf{u}}_{||} + 2(h_y\hat{u}_z - h_z\hat{u}_y)\mathbf{e}_y)\left(1+\frac{i}{q_2}\right)e^{iq_2} \quad \text{(A2)}$$

for a field point in the xy plane. We see that $\mathbf{b}$ is in the xy plane, as it should be. Here, we have

$$\mathbf{q}_{1,||} = (\bar{x}, \bar{y} - h_y, 0), \quad \text{(A3)}$$

$$\hat{\mathbf{u}}_{||} = (\hat{u}_x, \hat{u}_y, 0). \quad \text{(A4)}$$

REFERENCES

[1]K. H. Drexhage, in *Progress in Optics*, edited by E. Wolf (North-Holland, Amsterdam, 1974), Vol. XII, p. 163.
[2]R. R. Chance, A. Prock, and R. Silbey, Adv. Chem. Phys. **39**, 1 (1978).
[3]J. B. Pendry, Phys. Rev. Lett. **85**, 3966 (2000).
[4]J. A. Girón, J. R. Mejía-Salazar, J. C. Granade, and O. N. Oliveira, Jr., Phys. Rev. B **94**, 245430 (2016).
[5]F. J. Rodríguez, M. F. Picardi, and A. V. Zayats, Phys. Rev. B **97**, 205401 (2018).
[6]H. F. Arnoldus and Z. Xu, J. Opt. Soc. Am. B **36**, F18 (2019).
[7]H. F. Arnoldus and J. T. Foley, Opt. Commun. **231**, 115 (2004).
[8]X. Li, J. Shu, and H. F. Arnoldus, Opt. Lett. **33**, 2269 (2008).
[9]X. Li and H. F. Arnoldus, Phys. Lett. A **374**, 1063 (2010).
[10]D. Haefner, S. Sukhov, and A. Dogariu, Phys. Rev. Lett. **102**, 123903 (2009).
[11]D. Meschede, W. Jhe, and E. A. Hinds, Phys. Rev. A **41**, 1587 (1990).
[12]R. M. Amos and W. L. Barnes, Phys. Rev. B **55**, 7249 (1997).
[13]H. B. G. Casimir and D. Polder, Phys. Rev. **73**, 360 (1948).
[14]G. Barton, J. Phys. B At. Mol. Opt. Phys. **7**, 2134 (1974).
[15]H. Morawitz, Phys. Rev. **187**, 1792 (1969).
[16]G. Barton, Proc. R. Soc. London Ser. A **320**, 251 (1970).
[17]M. Babiker and G. Barton, Proc. R. Soc. London A **326**, 255 (1972).
[18]M. R. Philpott, Chem. Phys. Lett. **19**, 435 (1973).
[19]P. W. Milonni and P. L. Knight, Opt. Commun. **9**, 119 (1973).
[20]R. R. Chance, A. Prock, and R. Silbey, J. Chem. Phys. **62**, 771 (1975).
[21]W. Jhe, Phys. Rev. A **43**, 5795 (1991).
[22]W. Jhe, Phys. Rev. A **44**, 5932 (1991).
[23]T. Kobayashi, Q. Zheng, and T. Shekiguchi, Phys. Lett. A **199**, 21 (1995).
[24]A. G. Vaidyanathan, W. P. Spencer, and D. Kleppner, Phys. Rev. Lett. **47**, 1592 (1981).
[25]R. G. Hulet, E. S. Hilfer, and D. Kleppner, Phys. Rev. Lett. **55**, 2137 (1985).
[26]W. Jhe, A. Anderson, E. A. Hinds, D. Meschede, L. Moi, and S. Haroche, Phys. Rev. Lett. **58**, 666 (1987).
[27]X. Li and H. F. Arnoldus, Phys. Rev. A **81**, 053844 (2010).
[28]X. Li and H. F. Arnoldus, Opt. Commun. **305**, 76 (2013).
[29]Z. Xu and H. F. Arnoldus, J. Mod. Opt. **64**, 2123 (2017).
[30]H. F. Arnoldus and Z. Xu, J. Adv. Opt. Photon **1**, 143 (2018).
[31]S. C. Skipsey, G. Juzeliunas, M. Al-Amri, and M. Babiker, Opt. Commun. **254**, 262 (2005).
[32]J. D. Jackson, *Classical Electrodynamics*, 3rd ed. (Wiley, New York, 1999), p. 411.